Efficient Full-Wave Simulation in Layered, Lossy Media

Sharad Kapur* David E. Long* Jinsong Zhao†

* Bell Laboratories, Lucent Technologies, Murray Hill, NJ 07974
† University of California, Santa Cruz, CA 95064

Abstract

We describe a fast integral equation-based method for full-wave extraction in layered media. The method uses a combination of the fast integral equation solver IES^3, layered Green's functions, and a formulation that gives a well-conditioned linear system even in the "electrically-small" regime (i.e., when circuit structures are a fraction of the wavelength of light). The overall approach gives $O(N \log N)$ complexity, where N is the number of panels in a discretization of the conductor surfaces. We apply our method to the simulation of an integrated inductor on a lossy CMOS substrate and compare the results to measurement.

I. Introduction

Extraction and simulation of passive components play a significant role in the design of modern RF ICs. Increasing frequencies have made "full-wave" simulation critical for components that may be operated near resonance. General purpose field solvers based on finite-difference or finite-element schemes (e.g., Ansoft and HP-HFSS) can be used. However, they require volume discretization, resulting in large computation time and memory use, and it is difficult to enforce radiating boundary conditions for open regions. Simulation tools based on layered media integral equation formulations (such as HP-Momentum and Sonnet) are popular in the microwave and antenna communities. However, these tools employ direct solution methods which restricts them to small problems. In addition, the formulations that they are based on become ill-conditioned at lower frequencies, resulting in numeric difficulties. More recently, an integral equation formulation was combined with the precorrected FFT method for the efficient solution of electromagnetic problems [9]. While the algorithm is fast, it is likely to be applicable only to electrically large structures. More importantly, since it has not been combined with a layered media Green's function, it does not capture dielectric variation in the layers and loss in the substrate.

In this paper we present a general purpose full-wave electromagnetic analysis tool for the rapid simulation of passive structures in layered, lossy media. An integral equation formulation is used whereby all layered effects are captured by Green's functions [7], [8], [14]. A Galerkin-like scheme is used with basis functions that are composed of linear subsectional rooftop functions [10]. Ill-conditioning at low frequencies is avoided by choosing an appropriate mix of curl-free and divergence-free basis functions. The good conditioning, together with the fact that typical Green's functions vary smoothly with distance, are exploited using the fast integral equation solver IES^3 [6]. The result is an efficient algorithm for full-wave extraction. For typical problems, IES^3-based full-wave simulation is only about five times slower than IES^3-based capacitance extraction for the same structure. We demonstrate the speed and accuracy of our approach by simulating an integrated inductor on a lossy CMOS substrate and comparing the results to measurement.

II. Formulation

For the purposes of this paper, we will assume a "two-and-a-half dimensional" setup, with thin conductors characterized by a surface conductivity σ. If we assume a time-harmonic steady-state solution, then in frequency domain, the electric field $\mathbf{E}$ is expressed in terms of the vector potential $\mathbf{A}$ and the scalar potential ϕ:

$$\mathbf{E}(\mathbf{r}) = \mathbf{E}_{\rm inc}(\mathbf{r}) - j\omega\mathbf{A}(\mathbf{r}) - \nabla\phi(\mathbf{r}). \tag{1}$$

$\mathbf{E}_{\rm inc}$ is an incident (stimulus) field. The vector and scalar potentials are obtained by integrating over the conductor surfaces:

$$\mathbf{A}(\mathbf{r}) = \int_S \mathbf{G}^{\mathbf{A}}(\mathbf{r},\mathbf{r}')\mathbf{J}(\mathbf{r}')dS', \tag{2}$$

and

$$\phi(\mathbf{r}) = \int_S G^{\phi}(\mathbf{r},\mathbf{r}')\rho(\mathbf{r}')dS'. \tag{3}$$

$\mathbf{J}$ is the surface current density, ρ is the surface charge density, $\mathbf{G}^{\mathbf{A}}$ is the (dyadic) vector potential Green's function, and G^{ϕ} is the scalar potential Green's function. In free space

$$\mathbf{G}^{\mathbf{A}}(\mathbf{r},\mathbf{r}') = \frac{\mu_0}{4\pi}\frac{e^{-j\omega|\mathbf{r}-\mathbf{r}'|/c}}{|\mathbf{r}-\mathbf{r}'|}\mathbf{I} \tag{4}$$

$$G^{\phi}(\mathbf{r},\mathbf{r}') = \frac{1}{4\pi\epsilon_0}\frac{e^{-j\omega|\mathbf{r}-\mathbf{r}'|/c}}{|\mathbf{r}-\mathbf{r}'|}, \tag{5}$$

where c is the speed of light and ϵ_0 and μ_0 are the permittivity and permeability of vacuum. In a layered medium, analytic expressions for the Green's functions do not exist. However, there are a number of numerical approaches for computing them [7], [8], [14]. The layered media Green's functions are briefly discussed in Section IV. The current density $\mathbf{J}$ is related to the charge density ρ by

$$\nabla_S \cdot \mathbf{J}(\mathbf{r}) + j\omega\rho(\mathbf{r}) = 0. \tag{6}$$

At the surface of a conductor, the current density is given by $\mathbf{E} = \mathbf{J}/\sigma$. Combining this relation with Equation (1) yields

$$\frac{\mathbf{J}(\mathbf{r})}{\sigma} = \mathbf{E}_{\rm inc}(\mathbf{r}) - j\omega\mathbf{A}(\mathbf{r}) - \nabla\phi(\mathbf{r}). \tag{7}$$

Equations (7) and (6) are used to solve for the current **J**.

For the numerical solution of the equations, the structure is discretized into triangular elements [12], and a method of moments Galerkin-type scheme is used [4]. The individual basis functions are composed of Rao-Wilton-Glisson subsectional rooftop functions [10]. In their formulation, pairs of rooftop functions are used to represent the current flow across each interior edge in the discretization. At high frequencies this gives good results, but there are serious ill-conditioning problems at low frequencies. (By low frequency, we mean that the size of the structure is a small fraction of a wavelength.) This fact has been noticed by a number of authors [2], [8], [13]. The ill-conditioning arises because the scalar potential ϕ becomes numerically dominant at low frequencies. Without special precautions, the vector potential contributions are swamped, and inverting the matrix would require reconstructing **J** only from its divergence. While this ill-conditioning causes a loss of accuracy for direct factorization methods, for typical frequencies of interest in RF IC applications it is usually not fatal. However, it obviates the use of iterative methods, since their performance is strongly dependent on the conditioning of the linear system.

In order to avoid this ill-conditioning, we adopt a set of basis functions that decompose the current density into divergence-free and curl-free parts. This approach is similar to that taken by other authors [8], [13]. The divergence-free basis functions represent current loops. Hence they do not contribute to the scalar potential, and they are not affected by it. As a result, the linear system decouples at low frequencies, with the equations corresponding to the loops representing a magnetostatic problem. The basis functions are generated by first constructing a graph G whose nodes are elements of the discretization and whose edges represent connections between elements. We then find a spanning tree T and a cycle basis C [5] for G. The curl-free basis functions are composed of pairs of rooftop functions that represent current flow across edges in T. Each loop in C gives rise to a divergence-free basis function. Expanding the current **J** using the basis functions and testing against the same functions in the standard fashion [4], [13] gives a linear system $Bx = s$, where x is the vector of basis function coefficients and s is the stimulus.

III. Rapid Matrix Solution

Direct solution of the linear system $Bx = s$ via Gaussian Elimination requires $O(N^2)$ storage and $O(N^3)$ time, where N is the dimension of B. This is the approach used by conventional tools like HP-Momentum and Sonnet. However, the cubic complexity makes this approach impractical for large problems. By formulating the problem with separate curl-free and divergence-free components, the condition number is small and grows slowly with problem size. Hence, Krylov-subspace iterative schemes such as GMRES [11] or QMR [3] can be used. Iterative solvers require application of the matrix B to a sequence of recursively generated vectors. The dominant costs become the $O(N^2)$ time and space required for constructing and storing the matrix and the $O(N^2)$ time required for each matrix-vector product. While this is already an improvement over direct factorization, the storage and computational cost is still excessive. Each of these costs can be reduced to $O(N \log N)$ for typical problems using the fast integral equation solver IES^3 [6].

The key idea behind IES^3 is to exploit the fact that typical Green's functions vary smoothly with distance. Consequently, large parts of the matrix B are numerically low-rank. These low-rank regions are represented as sparse outer products using the singular value decomposition (SVD). The SVD is an extremely effective tool for the compression of rank deficient matrices. Based on this observation, Kapur and Long [6] describe a scheme for recursively partitioning, sampling and compressing the matrix. Figure 1 is a "rank map" of a matrix corresponding to the inductor described in Section V. The rank map shows the partitioning of the matrix into submatrices and the rank of each submatrix. Although there are some strong off-diagonal interactions, the rank map is typical in problems where the time and memory requirements drop from $O(N^2)$ to $O(N \log N)$.

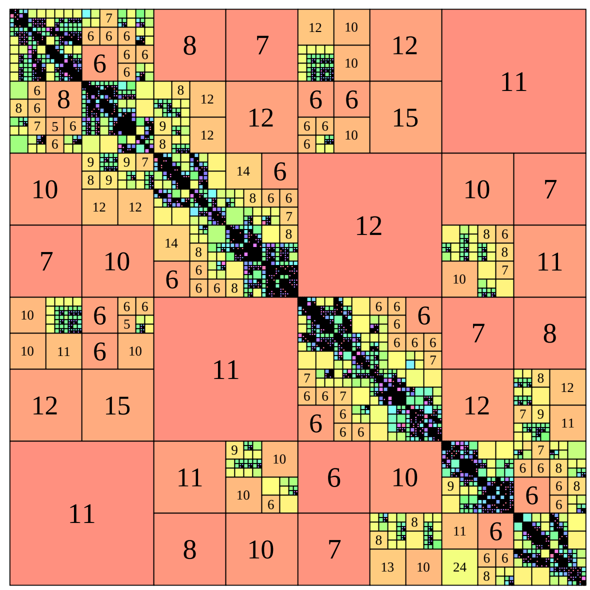

Fig. 1. Rank map of a method-of-moments matrix for the inductor of Section V

IV. Layered Media Green's functions

RF passive components are often fabricated in a layered dielectric medium. Fortunately, layered Green's functions can easily be combined with the above formulation to account for dielectric layer variation and loss [1], [7], [8], [14]. Layered Green's functions decouple the process structure from the circuit geometry and can be precomputed, compressed and stored. Once the process variables are fixed, the Green's functions remain unchanged for each new extraction. It can be shown that the spectral-domain full-wave layered Green's function can be derived from the solution of three decoupled one-dimensional wave equations [1], [7], [14]. These one-dimensional wave equations can be easily solved analytically. The resulting spectral-domain Green's function must then be numerically transformed into space domain. Details of these procedures are involved and can be found in the microwave literature [1], [7], [8], [14].

We use the procedure described in [14] to efficiently compute these space domain Green's functions. The results of the computation are tabulated in a database off-line. Building the database for a given process takes a few minutes. Evaluating a single interaction between a source and observation pair takes about twice as long as evaluating the free-space Green's function for the pair.

V. Experimental Results

The simulator has been run on a number of examples, including capacitors, inductors, and filters on CMOS and MCM substrates. In this section, we report simulation results for an integrated inductor on a highly conductive CMOS substrate. The layout is shown in Figure 2. The inductor is constructed with the top two metal layers of the process.

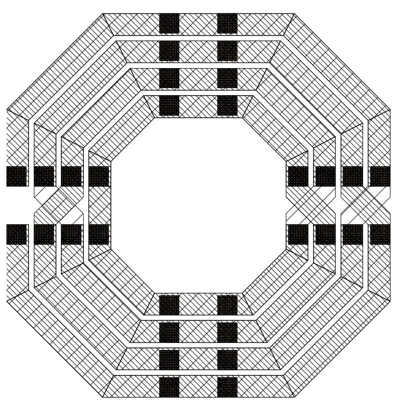

Fig. 2. CMOS inductor layout

For measurement purposes, the inductor was connected to a pad frame, and the same pad frame was included in the simulation to avoid uncertainties associated with de-embedding. The pads connected to one of the inductor terminals were grounded, and the single-port S parameter looking into the other pad was measured. This S parameter was converted into a complex impedance. Comparisons between the simulation results and measurement are shown in Figure 3. The graphs show the magnitude and phase of the complex impedance, and also the ratio of imaginary to real parts, which represents a quality factor Q for the inductor. The simulation predicts a slightly higher quality factor, but the discrepancy is well within the process variation. (Nominal values for all process parameters were used in the simulation.)

We also examined the performance of the simulator as the discretization level was increased. The results are show in Figure 4. These simulations were of the inductor alone (no pads) for a single frequency of 3 GHz. Discretization sizes ranged from 1,500 elements to 11,500 elements, yielding matrix sizes of between 2,000 and 16,000 (the difference is the number of divergence-free basis functions). The graphs show the total CPU time and the number of nonzeros in the compressed matrix representation. Both time and memory scale slightly faster than linearly as the system size grows. Almost all of the time goes into building the compressed matrix representation. The iterative solve, which is preconditioned using a sparse matrix that captures only the nearby interactions, required no more than thirty iterations at any discretization level to achieve a relative reduction of 10^4 in the norm of the residual. The smallest simulation took about four minutes, and the largest required about fifty minutes. The total simulation times compare favorably to the time required for extracting only the parasitic capacitance of the same inductor. At the highest discretization level, our IES^3-based capacitance extractor [6] using the same Green's functions requires ten minutes. Note that in the full-wave case, a triangle with three neighbors requires four integrals: one for computing the scalar potential, and one for each edge when computing the vector potential. Since each vector potential integral also involves manipulating vectors rather than scalars, the factor of five difference in time is about the best that can be expected.

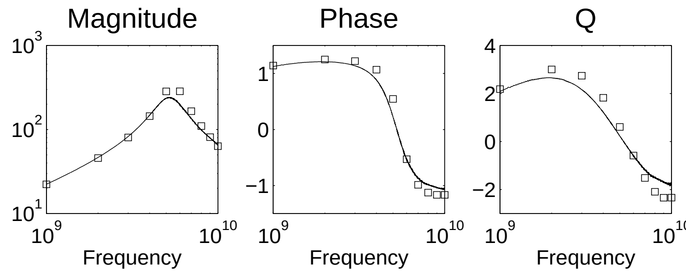

Fig. 3. Comparison of simulation (boxes) to measurement (lines)

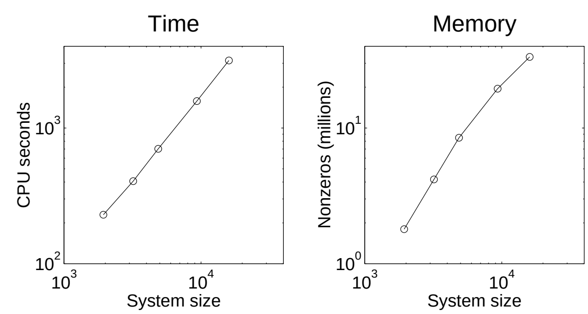

Fig. 4. Time and memory requirements

The convergence of Q (which is the most sensitive parameter computed from the simulation) as the discretization level is increased is shown in Figure 5. Low discretization levels tend to overestimate Q since current crowding effects are missed.

Results from the simulation can also be used to gain intuition about how the inductor is operating. The current distribution in one section of the inductor is shown in Figure 6. Light areas in the figure indicate higher current density. It is clear that significant current crowding occurs in the innermost turn.

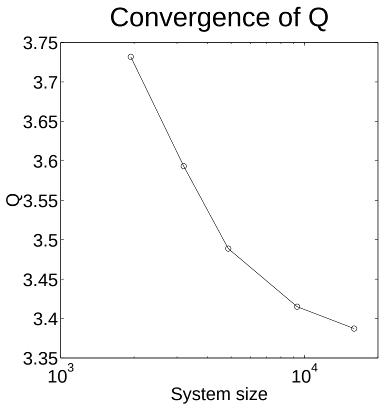

Fig. 5. Convergence behavior with increasing discretization

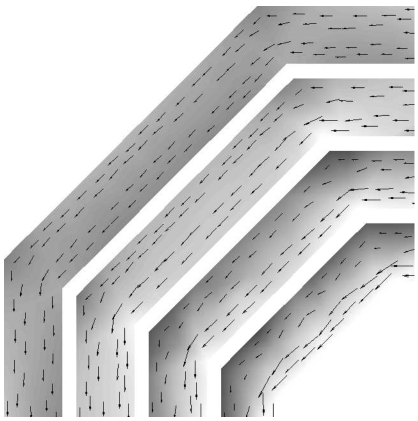

Fig. 6. Current flow in the inductor

Even though the simulation only solves for the current density in the conductors, we can use the layered Green's functions and Equation (1) to obtain the eddy currents that are induced in the conductive substrate. We do this by computing the substrate electric field arising from the conductor currents and then multiplying by the substrate conductivity. A cross section of the substrate together with the current density is shown in Figure 7. Nontrivial currents penetrate the substrate to depths on the order of one hundred microns.

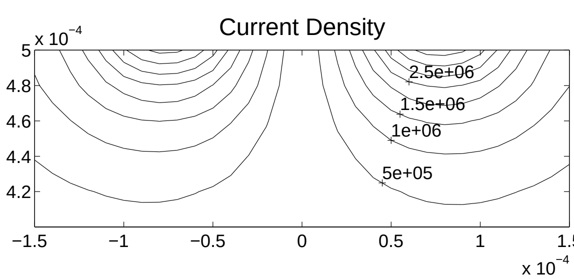

Fig. 7. Cross section of substrate showing eddy currents

VI. Conclusion

We described a general purpose full-wave electromagnetic analysis tool for the simulation of passive structures in layered, lossy media. The formulation is based on integral equations using layered Green's functions to capture the effects of the medium. The conductor current distribution is decomposed into curl-free and divergence-free parts in order to avoid ill-conditioning. An $O(N \log N)$ solution procedure is obtained by constructing and compressing the method-of-moments matrix using IES^3 [6] together with an iterative solver. For typical problems, IES^3-based full-wave simulation is only about five times slower than capacitance extraction for the same structure. Simulation results were presented for an integrated inductor on a lossy CMOS substrate. The results compare favorably to measurements.

Acknowledgements

We thank Peter Kinget and Andrew Becker for the inductor example.

References

[1] W. C. Chew. *Waves and Fields in Inhomogenous Media*. IEEE Press, New York, 1995.

[2] D.R.Wilton and A. Glisson. On improving the stability of the electric field integral equation at low frequency. In *IEEE AP-S National Symposium*, pages 124–133, Los Angeles, June 1981. IEEE.

[3] R. W. Freund and N. M. Nachtigal. QMR: A quasi-minimal residual method for non-Hermitian linear systems. *Numerishce Mathematik*, 60:315–339, 1991.

[4] R. F. Harrington. *Field Computation by Moment Methods*. IEEE Press, New York, 1991.

[5] J. D. Horton. A polynomial-time algorithm to find the shortest cycle basis of a graph. *SIAM J. Comput.*, 16(2):358–366, Apr. 1987.

[6] S. Kapur and D. E. Long. IES^3: A fast integral equation solver for efficient 3-dimensional extraction. In *37th International Conference on Computer Aided Design*, Nov 1997.

[7] K. Michalski and J. Mosig. Multilayered media Green's functions in integral equation formulation. *IEEE Transaction on Antenna and Propagation*, 45(3):508–519, March 1997.

[8] J. Mosig and F. Gardiol. Analytic and numerical techniques in the Green's function treatment of microstrip antennas and scatterers. In *Inst. Elect. Eng. Proc.*, volume 130, pages 175–182, March 1983. Pt. H.

[9] J. R. Philips, E. Chiprout, and D. Ling. Efficient full-wave electromagnetic analysis via model-order reduction and fast integral transforms. In *34th Design Automation Conference*, June 1996.

[10] S. M. Rao, D. Wilton, and A. Glisson. Electromagnetic scattering by surfaces of arbitrary shape. *IEEE Transactions on Antenna and Propagation*, AP-30:409–418, May 1982.

[11] Y. Saad and M. H. Shultz. GMRES: A generalized minimal residual algorithm for solving nonsymmetric linear systems. *SIAM Journal on Scientific and Statistical Computing*, 7(3):856–869, July 1986.

[12] J. R. Shewchuk. Triangle: Engineering a 2D quality mesh generator and Delaunay triangulator. In *First Workshop on Applied Computational Geometry*, pages 124–133. Association for Computing Machinery, May 1996.

[13] S. Uckun, T. K. Sarkar, S. M. Rao, and M. Salazar-Palma. A novel technique for analysis of electromagnetic scattering from microstrip antennas of arbitrary shape. *IEEE Transactions on Microwave Theory and Techniques*, 45(4):485–491, Apr. 1997.

[14] J. Zhao, S. Kapur, and D. E. Long. Efficient three-dimensional extraction based on static and full-wave layered Green's functions. Submitted for publication.